AD-A135 951 STATUS OF LIGHT ION INERTIAL FUSION RESEARCH AT NRL (NAVAL RESEARCH LABORATORY)(U) NAVAL RESEARCH LAB WASHINGTON DC G COOPERSTEIN ET AL. 30 NOV 83 1/1

UNCLASSIFIED NRL-MR-5219 F/G 20/7 NL

END

FILMED

DTIC

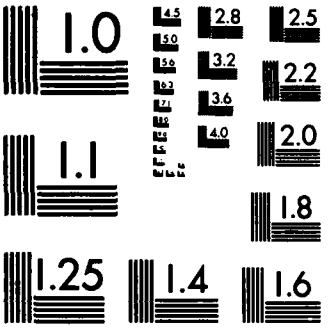

MICROCOPY RESOLUTION TEST CHART
NATIONAL BUREAU OF STANDARDS-1963-A

NRL Memorandum Report 5219

Status of Light Ion Inertial Fusion Research at NRL

G. COOPERSTEIN, P. F. OTTINGER,* SHYKE A. GOLDSTEIN,*
R. J. BARKER,** D. G. COLOMBANT, R. A. MEGER,* J. M. NERI,*
D. MOSHER, F. L. SANDEL,* S. J. STEPHANAKIS AND F. C. YOUNG

Plasma Technology Branch
Plasma Physics Division

**JAYCOR, Inc.*
Alexandria, VA 22304

***Mission Research Corporation*
Alexandria, VA 22312

November 30, 1983

This report was presented at the Sixth International Workshop on Laser Interaction and Related Plasma Phenomena, October 25-29, 1982, Monterey, CA.

This research was sponsored in part by the Department of Energy and the Defense Nuclear Agency under Subtask T99QAXLA014, work unit 00023 and work unit title "Status of Light Ion Inertial Fusion Research at NRL."

NAVAL RESEARCH LABORATORY
Washington, D.C.

SECURITY CLASSIFICATION OF THIS PAGE (When Data Entered)

REPORT DOCUMENTATION PAGE

READ INSTRUCTIONS BEFORE COMPLETING FORM

1. REPORT NUMBER: NRL Memorandum Report 5219	2. GOVT ACCESSION NO. AD-A135 951
3. RECIPIENT'S CATALOG NUMBER	
4. TITLE (and Subtitle): STATUS OF LIGHT ION INERTIAL FUSION RESEARCH AT NRL	5. TYPE OF REPORT & PERIOD COVERED: Interim report on a continuing NRL problem.
	6. PERFORMING ORG. REPORT NUMBER
7. AUTHOR(s): G. Cooperstein, P.F. Ottinger,* Shyke A. Goldstein,* R.J. Barker,** D.G. Colombant, R.A. Meger,* J.M. Neri,* D. Mosher, F.L. Sandel,* S.J. Stephanakis and F.C. Young	8. CONTRACT OR GRANT NUMBER(s)
9. PERFORMING ORGANIZATION NAME AND ADDRESS: Naval Research Laboratory, Washington, DC 20375	10. PROGRAM ELEMENT, PROJECT, TASK AREA & WORK UNIT NUMBERS: DE-AI08-79DP40092; 47-0879-0-3; 47-0875-0-3 see back
11. CONTROLLING OFFICE NAME AND ADDRESS: Department of Energy, Washington, DC 20545; Defense Nuclear Agency, Washington, DC 20305	12. REPORT DATE: November 30, 1983
	13. NUMBER OF PAGES: 26
14. MONITORING AGENCY NAME & ADDRESS(if different from Controlling Office)	15. SECURITY CLASS. (of this report): UNCLASSIFIED
	15a. DECLASSIFICATION/DOWNGRADING SCHEDULE

16. DISTRIBUTION STATEMENT (of this Report)

Approved for public release; distribution unlimited.

17. DISTRIBUTION STATEMENT (of the abstract entered in Block 20, if different from Report)

18. SUPPLEMENTARY NOTES

*JAYCOR, Inc., Alexandria, VA 22304
**Mission Research Corporation, Alexandria, VA 22312
F.L. Sandel — Present address: Eastern Research Engineering, Alexandria, VA 22304

(Continues)

19. KEY WORDS (Continue on reverse side if necessary and identify by block number)

Intense ion beams	Ion beam transport
Pinch-reflex diode	Ion beam brightness
Inertial confinement fusion	Inductive energy storage
Ion beam focusing	Ion energy deposition

20. ABSTRACT (Continue on reverse side if necessary and identify by block number)

High-brightness proton beams have recently been extracted from axial pinch-reflex diodes (PRD) mounted on the NRL Gamble II generator. The source power brightness that was measured exceeded 10 TW/cm²rad². Analysis of a modular ICF system using such diodes shows that an operational window for transport of light-ion species exists. Multi-terawatt beams can be transported a few meters in channels a few centimeters in diameter. A proof-of-principle experiment for the required final focusing cell has been successfully carried out on Gamble II. A new barrel-shaped equatorial PRD that can be coupled

(Continues)

DD FORM 1 JAN 73 1473 EDITION OF 1 NOV 65 IS OBSOLETE
S/N 0102-014-6601

SECURITY CLASSIFICATION OF THIS PAGE (When Data Entered)

18. SUPPLEMENTARY NOTES (Continued)

This report was presented at the Sixth International Workshop on Laser Interaction and Related Plasma Phenomena, October 25-29, 1982, Monterey, CA.

This research was sponsored in part by the Department of Energy and the Defense Nuclear Agency under Subtask T99QAXLA014, work unit 00023 and work unit title "Status of Light Ion Inertial Fusion Research at NRL."

20. ABSTRACT (Continued)

to PBFA II as a single diode has also been operated on Gamble II and has demonstrated 50% ion efficiency with predominately azimuthally-symmetric charged-particle flow. Preliminary experiments using vacuum inductive storage and plasma opening switches have demonstrated factor-of-three pulse compressions, with corresponding power and voltage multiplications for pulse durations of interest to PBFA II. In other experiments the stopping power of deuterons in hot plasmas was measured. Results show about 40% enhancement in stopping power over that in cold targets when the deuteron beam is focused on the target to about 0.25 MA/cm2.

Sq cm.

CONTENTS

STATUS OF LIGHT ION INERTIAL FUSION RESEARCH AT NRL

I. INTRODUCTION

In the past few years there has been great interest in using light-ion beams to drive thermonuclear pellets. Terrawatt-level ion beams have been efficiently produced using conventional pulsed power generators at Sandia National Laboratory (SNL) with magnetically-insulated ion diodes[1,2] and at the Naval Research Laboratory (NRL) with pinch-reflex ion diodes (PRDs).[3] In addition, extensive experimental[4] and theoretical[5] work has been reported concerning focusing and transport of such beams for a multimodule light-ion inertial confinement fusion (ICF) scheme. Here more recent work at NRL is reviewed involving investigation of different ignition-system configurations for PBFA II, including the development of inductive storage techniques using fast plasma opening switches, and a new barrel shaped equatorial pinch-reflex diode. In addition, experiments designed to study enhanced stopping of high current density ion beams will also be reviewed.

Recent NRL experiments and theory have involved the investigation of key aspects of three ignition-system configurations for light-ion drivers on PBFA II at SNL. The first configuration uses the traditional NRL multimodular approach where a number of modules are used to drive small-area disc-like axial PRDs each of which focuses a 50 ns, 5 MeV proton beam into its own Z-discharge transport channel about 2 m long and a few cm in diameter.[5] Each channel is terminated in a short, higher-current discharge which magnetically focuses the beam onto the pellet. In previous work at NRL,[6] the beam was first focused to pellet diameter before being transported. The small channel diameter limited transportable energy to a fraction of a MJ per channel. The present larger diameter channels coupled with final focusing sections should allow each channel to transport more than 1 MJ, thus reducing the number of channels required to drive a pellet.[7]

The second configuration being studied ties 36 modules of PBFA II to a single barrel-shaped radial pinch-reflex ion diode surrounding the pellet located at the diode center.[3,8,9] For reasons which will be evident this new diode is called the equatorial pinch-reflex diode (EPRD). The barrel diameter (~1m) must be small enough to permit focusing to pellet dimensions but large enough to permit time-of-flight bunching of the beam from the power-pulse duration to the pellet driving time.

The third configuration being studied ties the 36 modules together into some smaller number of lines and utilizes vacuum inductive storage techniques and plasma opening switches[10] to compress the power pulse to the 10 to 15 ns pellet driving time. The modules can then be used to drive a multimodule system or combined to power a single diode. The power in the system is correspondingly increased by voltage multiplication. Higher voltage allows the use of heavier ions such as singly charged lithium. Thus, the higher voltage, shorter pulse duration, and heavier ion mass should more easily allow the production of ion beams of the necessary brightness for focusing to pellet

Manuscript approved September 15, 1983.

dimensions. Only the second and third single-diode configurations are compatible with imploding foil experiments planned for PBFA II,[2] while only the first configuration is compatible with a repetitively pulsed reactor system. Some of the important results obtained at NRL while investigating these three configurations are introduced below and will be discussed in more detail in the sections that follow.

High-brightness proton beams (0.4 MA, 1 MV) have recently been extracted from 20 cm^2 axial PRDs mounted on Gamble II. A source power brightness of $\geq$ 10 TW/cm^2rad^2 was achieved by minimizing the vacuum gap between the anode and cathode-transmission foils, thereby reducing the disruptive effects of filamentation in the vacuum gap.[11] Stability constraints have recently been combined with channel-MHD and energy-loss constraints to define an operational window for transport of high power beams of various light-ion species produced from such diodes.[7] Calculations of two-stream- and filamentation-instability growth rates show that multi-terawatt beams can be transported a few meters in channels a few centimeters in diameter. Less than 10 channels would be sufficient to transport PBFA-II level beams and ignite a pellet provided that final magnetic focusing can be utilized to focus each transported beam.[5] A proof-of-principle experiment for final focusing has been successfully carried out on Gamble II using a 100 kA discharge channel 4 cm in diameter and 8 cm long mounted immediately outside of the diode.[12,13] Experiments in which a transported beam will be focused are planned.

Barrel-shaped EPRD experiments on Gamble II operating at 1.2 MV and 0.8 MA have demonstrated 50% proton efficiency with predominately azimuthally-symmetric charged-particle flow, average beam-divergence half-angles in the 1-2° range between filaments, and good agreement with theoretical scaling laws.[8] This low divergence could lead to a very interesting high brightness ion beam. A high-power diode of similar design is now being tested on PBFA-I.[9]

The first experimental results using vacuum inductive storage and plasma opening switches have been obtained on the NRL Gamble I generator.[10] This work is an extension of the efforts at Sandia National Laboratories where plasma erosion switches were used for prepulse suppression and sharpening pulse risetime.[14] The switch has been shown to conduct up to 200 kA of current for ~ 50 ns and then to open in < 10 ns, transferring the current to an electron-beam load. Inductive storage, pulse compression, and voltage and power multiplication have been demonstrated. A simple model explaining the switch operation has been developed.

Other experiments on Gamble II have employed 20 cm^2 axial PRDs to measure the energy loss of deuteron beams in subrange Mylar and aluminum targets located at the beam focus.[15] These targets were sandwiched between thin CD_2 layers so that ion-energy loss could be determined from time-of-flight analyses of the two

neutron pulses. Results show about 40% enhancement in stopping power over that in cold targets when the beam was focused to about 0.25 MA/cm^2 on the target. Results of these and other lower-current-density measurements are in excellent agreement with calculated stopping due to free and bound electrons at ionization levels expected from ion-target heating.[16] Factor-of-two enhancements over cold stopping for light- and heavy-ion beams are predicted at target temperatures expected for break-even pellets.

Section II of this paper discusses the modular approach to light-ion ICF with the results of recent ion brightness studies on axial pinch reflex diodes being reviewed in Sec. 2.1. The transport of ion beams in large diameter channels is discussed in Sec. 2.2 and the use of final focusing sections to compress the transported beams to pellet dimensions is discussed in Sec. 2.3. Section III of the paper describes the single diode approach to light-ion ICF using the barrel-shaped EPRD, and the pulse compression approach using inductive storage techniques with plasma opening switches is discussed in Sec. IV. The results of deuteron stopping experiments in hot plasmas is reviewed in Sec. V, and, finally, Sec. VI outlines future plans.

II. MODULAR APPROACH

Up to the present, the main NRL approach to light-ion ICF has been to consider using PBFA II to drive two or more separate pinch-reflex ion diodes each with its own transport system as illustrated in Fig. 1. A small diameter pinch-reflex ion diode produces the ions and properly aims them towards the transport system entrance aperture. The ion beam then free streams in a gas-filled focusing drift region towards a $\geq$ 1 cm diameter focus. The gas in the drift region allows the ion beam to be

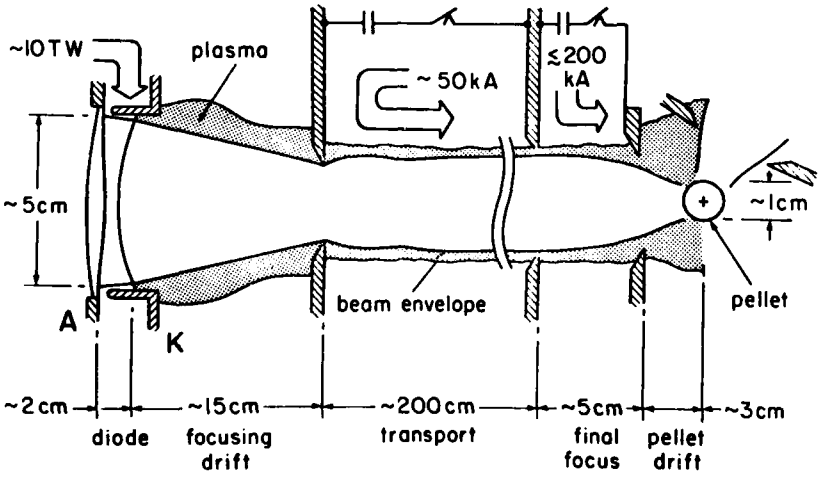

Fig. 1. Schematic of one module of a multimodule ICF system.

highly charge- and current-neutralized. Inside the channel, the ions are confined radially by the azimuthal magnetic field produced by the discharge of an external capacitor bank. The current in the channel confines ions entering the channel typically with transverse velocities below about 15% of their axial velocity. The plasma density in the channel must be sufficiently high to provide inertial resistance to channel expansion forces during beam transit and sufficiently low to prevent excessive energy loss of the beam during transport. Beam power multiplication of about a factor of five is achieved during transport to the pellet by ramping the accelerator voltage in time. After transport, the ion beam will be further focused to pellet dimensions by passing through a short, higher current, plasma channel whose length is between 1/8 and 1/4 of an ion betatron wavelength. Several of these modules will surround the pellet. The purpose of the final focus cell is to allow larger diameter channels to be used for transport and bunching. This, in turn, will allow the transport of higher power ion beams, thus reducing the number of channels needed for PBFA II to between 2 and 10. The following three subsections will describe recent results in the areas of ion production, transport, and final focusing.

2.1 ION BEAM BRIGHTNESS STUDIES

Beam power brightness at the diode imposes the ultimate limit on the ability to focus ion beams onto targets. The PRD, which has been previously described[6] and which is illustrated in Fig. 2, is being studied with respect to its performance as a source of high current density, low divergence ion beams. In the past it

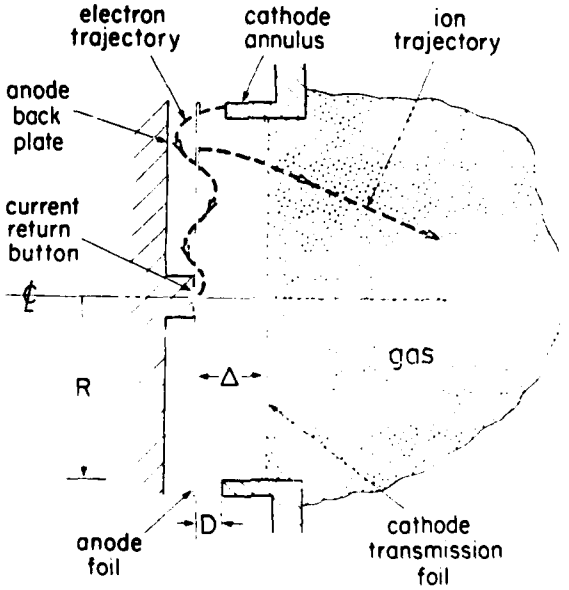

Fig. 2. Schematic of a pinch-reflex diode (PRD).

has been reported that 0.5 TW deuteron beams produced from PRDs on the NRL Gamble II generator were focused to peak current densities of about 300 kA/cm^2 which corresponds to a power brightness of about 2 TW/cm^{2}rad^2.[6] Similar diodes have produced nearly 2 TW, 100 kJ proton and deuteron beams with 60% ion production efficiency on the Physics International PITHON generator.[17] Recent NRL experiments have demonstrated that considerably brighter beams are attainable. Both experimental and theoretical efforts are involved in the new work. Electron-filamentation instabilities which may occur in the electrode plasmas[18] and vacuum gap[19] are currently under investigation. Small-scale perturbations in diode electromagnetic fields associated with such instabilities can degrade brightness. In addition to their effects on beam brightness, varying electromagnetic fields and electrode-plasma motion also introduce time-dependent aberrations in the focusing properties of the diode. Changes in diode geometry and electrode materials are being investigated experimentally in order to determine their effects on the instabilities.

Provided that ion efficiency is not reduced and beam-divergence is not degraded, diode-beam brightness can be increased by reducing the diode radius. This was demonstrated in recent 1 TW diode experiments on Gamble II, where 0.6 TW proton beams were extracted from small 20 cm^2-area anode foils.[11] The ion beam brightness was measured crudely by a shadowbox technique that uses multiple pinhole images of the ion beam. The recording plates used were either brass or heat sensitive plastic. The brass is heated up by the impinging ion beam causing zinc to collect on the surface. Small features of ion beamlets can be clearly recorded provided their current density is high ($J_i \sim 10^3$ A/cm^2). The heat sensitive plastic is more sensitive and records current densities down to 10 A/cm^2. Using these plates with the multiple hole shadowbox mounted far enough from the diode, one can reconstruct the ion source pattern and its divergence. The ion source exhibited 10 to 20 beamlets for this small radius diode. Each beamlet had a size of about 1 cm in diameter. The beam divergence changed drastically when the gap, Δ, between the anode and the cathode inner foil was reduced. The half angle of the diverging beam cone, $\delta\theta$, was measured to be $\sim$ 0.1 rad at a gap of 1.5 cm and $\sim$ 0.05 rad at a gap of 0.5 cm. The divergence was observed as a conic structure with no preference to radial or azimuthal direction.

A simple calculation to explain beam divergence versus gap width was performed assuming that the total ion beam current (450 kA) was distributed equally among 15 sources each having a diameter of 1 cm. Self-pinching of these ion beamlets by self-magnetic fields would result in $\delta\theta = 0.08\Delta/\sqrt{V}$ for protons at a voltage V measured in MV. The experimental results at V = 1.2 MV show that $\delta\theta$ agrees well with the predicted value at the larger Δ of 1.5 cm. At the smaller gap the plasma motion from the cathode and anode reduce Δ from its initial value of 0.5 cm. The calculated divergence could then be as small as 0.015 rad compared

with the observed divergence of 0.05 rad. The larger experimental divergence cannot be explained by magnetic fields and must therefore be due to electric fields.

Two mechanisms have been identified for distortion of equipotentials. The first is associated with plasma hydrodynamics when the anode plasma is formed at discrete spots and expands in a two dimensional manner generating bulges on the anode. A 1-D hydrocode has been developed to model the axial expansion of the anode plasma.[20] Since the conductive anode plasma prevents electric field penetration, this 2-D expansion distorts the equipotential structure close to its surface. Such spotty structure is clearly seen in the shadowbox pinhole images and was also observed using interferometry on the PITHON experiment.[17] The second mechanism is electron beam filamentation in vacuum. The resultant space charge structure introduces azimuthal and radial components to the electric field in addition to the axial field.

The two mechanisms mentioned above would have caused large divergences ($\delta\theta \sim 0.2$ rad) if the electric field would have been compressed against the anode plasma where the ions are launched. The PRD, however, operates by screening the ion beam space charge with the relativistic electrons that pinch and reflex through the anode plasma. This action allows the equipotentials to be spread across the entire diode gap unlike the magnetically insulated diode that only operates at high ion current density when the equipotentials are pushed against the anode plasma. The observed lower $\delta\theta$ of 0.05 rad is a clear experimental demonstration that even at this average ion source current density of 20 kA/cm^2 the PRD is operating as a space charge enhanced source rather than an electric field enhanced source.

Recent focusing experiments were attempted with very small area curved anode foils (1.5 cm radius and 2.5 cm radius of curvature) in order to document very high current density focusing consistent with the measured ($\delta\theta \sim 0.05$ rad) intrinsic source divergence. Conducting structures were used to reduce the radial diode gap. In this way the smaller radial gap controlled the diode impedance while the axial gap could be set to a comfortable value to prevent premature gap closure. Similar structures have been used to allow up to twice the critical current to flow in pinched beam diodes.[21] The focusing region behind the 1.8 μm cathode foil was typically filled with 1 Torr of air. Measurements of K_α radiation showed an unexpected large area of radiation and shadowbox results revealed ion orbit bending near the focus. These experiments most likely indicate that there is a beam-plasma interaction in the focusing region resulting in a magnetic field structure which prevents good focusing. Different gases (air, He and Ar) at higher pressures are being used in the focusing region in order to resolve this problem.

The beam brightness ($JV/\delta\theta^2$) observed with 20 cm^2 area anode foils for V = 1.2 MV, J = 20 kA/cm^2 and $\delta\theta \sim$ 0.05 rad is ~ 10 TW/

cm^2rad^2. Scaling this figure up with voltage^2 to the 3 MV level and assuming a factor-of-4 bunching during transport without brightness loss, leads to a modular-beam brightness of about 250 TW/cm^2rad^2. If 40% of the solid angle surrounding a pellet is subtended by final-focus exit apertures, on target power densities approaching 100 TW/cm^2 might be achievable with proton beams from existing PRDs. Even higher power densities may be achievable with the higher beam brightness attainable with smaller radius diodes.

2.2 TRANSPORT

Intense light-ion beam transport in Z-discharge channels provides accelerator standoff from ICF targets and allows time-of-flight bunching of the beam to higher intensity. In the past, efficient transport of 100 kA-level ion beams over fe meter distances using Z-discharge plasma channels has been documented.[4,22] In addition, considerable work on th MHD response of the channel to the passage of intense bea as been reported,[23] as well as, extensive work on the stabili such beam-plasma systems.[24] Stability constraints combine th channel expansion and beam-energy-loss constraints have been used to define an operational window for efficient ion beam transport.[7] The stability constraints are derived from the requirements to avoid significant growth of the electron-ion beam two-stream instability, the beam-filamentation instability and the channel-filamentation instability. The channel-expansion constraint results from demanding that no significant $\tilde{J}\times\tilde{B}$ driven radial expansion of the channel occurs on the beam time scale. Finally, the beam-energy-loss constraint requires that no more than 25% of the beam energy is lost during transport.

The constraints have been derived for arbitrary beam-ion species in order to evaluate the advantages of higher-atomic-weight ions. The beam energy, beam radius and channel density are also free parameters which have been varied in order to determine their effects on the operational window. In all cases, the channel gas was taken as deuterium. This allows the use of a simple model for channel heating and has the advantage of reduced radial acceleration due to the passing beam at the same stopping power as hydrogen.

Results for beams of H^+, D^+, He^{+2} and C^{+6} show that a larger operational window exists for the higher-atomic-weight species. This is a consequence of their lower currents at equivalent transported power levels. Raising the channel density somewhat above the optimum for minimum beam energy loss during transport relaxes the two-stream and channel-filamentation stability constraints and the channel-expansion constraint while only slightly modifying the energy-loss constraint. Increasing the beam radius relaxes the two-stream stability constraint and considerably reduces the channel-expansion and beam energy-loss constraints.

From the above considerations it is determined that multi-terawatt beams can be transported a few meters in large-radius channels with beam divergence half angles of 0.1 to 0.2 radians. Such angles are presently attainable with PRDs. If time-of-flight bunching during transport and final focusing after transport are employed, less than 10 (and as few as 2) channels are required to deliver the power needed to ignite a pellet.

2.3 FINAL FOCUSING

Theoretical results[13] show that at least a factor-of-ten increase in final-focused ion-current density can be achieved for beams transported in hollow channels (i.e., channels with the discharge current flowing along the outer edge of the channel). Transport channels which carry the discharge current in the channel interior result in beam-brightness loss during transport and hence cannot be compressed as well by the final focusing cell. Focusing cells which are 1/8 of an ion-betatron-wavelength long focus the beam an additional 1/8-wavelength beyond the exit of the focusing cell. This 1-2 cm drift length is the stand-off distance separating the cell exit from the pellet. High plasma densities can be employed without excessive beam energy loss because of the short length of the focusing cell. The high density then minimizes the plasma-MHD response and, combined with a thin transmission foil at the exit of the cell, discourages pellet preheat from focusing-cell plasma plumes.

A final-focus system was designed and fielded on the Gamble II accelerator.[12] Figure 3 shows a schematic representation of the channel. A discharge of ~ 100 kA was initiated by an external capacitor bank along the Lexan insulator (shaded region in Fig. 3) which was filled with 5-10 Torr of air. Channel currents were

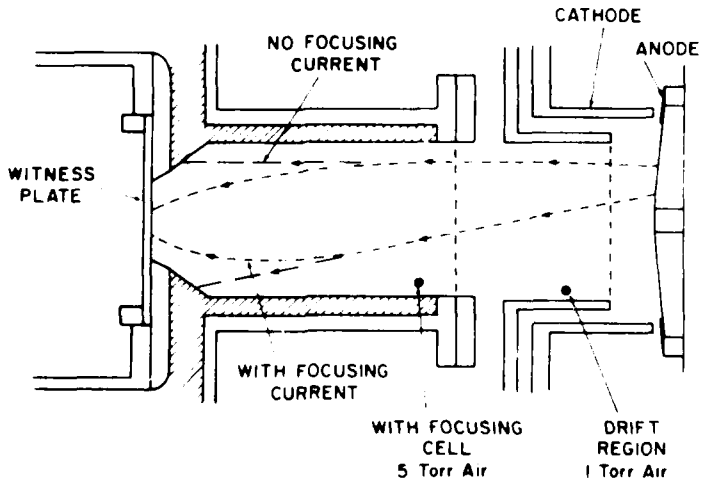

Fig. 3. Schematic of a final-focusing cell.

chosen to match a 1/4 betatron wavelength for the ions with the 8 cm channel length. No attempt was made in these early proof-of-principle experiments to synchronize the ion beam injection with the time dependent channel current density distribution. A convex pinch-reflex type anode was used to partially offset the self-pinching of the ion beam in the diode and provide a nearly parallel trajectory injected ion beam. When aluminum witness plates were used, rear surface spall only appeared over the aperture region when the focusing current was turned on. Further experiments with shadowboxes placed downstream of the aperture confirmed that no large scale mixing of the ion orbits in the 1/4 betatron wavelength focusing cell occurred during focusing. Further experiments where the channel current distribution is optimized for a given beam injection condition are planned. Eventually, experiments will be performed with a final-focusing system placed at the exit of the transport system.

III. SINGLE DIODE APPROACH

A new version of the NRL PRD has been designed to operate on the radial triplate geometry of PBFA-I. A conceptual schematic is shown in Fig. 4. This diode produces two cylindrically-symmetric

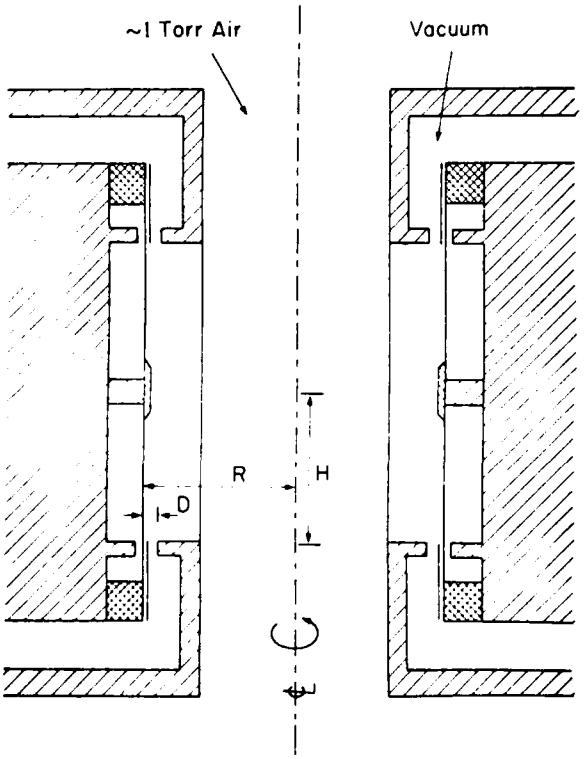

Fig. 4. Schematic of equatorial pinch-reflex diode (EPRD).

sheet beams of electrons which flow from top and bottom by self-magnetic pinching and reflexing action on the anode foil to a common line pinch around the equator of the diode, hence the name equatorial-pinch-reflex diode (EPRD).

Although this diode appears to be a simple topological variation of the conventional PRD, there are a number of basic conceptual differences. There is no electron-space-charge-density build-up at the center as occurs with the conventional axial PRD because there is no radially converging electron flow towards the diode axis. This lack of radial electron convergence leads to a constant ion current density rather than one that decreases inversely with the distance from the diode axis as in the axial PRD. These ions produce an azimuthal focusing magnetic field in the gap between the anode and cathode foils which increases proportionally to the distance from the equator. This, in turn, leads to a natural self-focusing of the ion beam even from a flat anode foil. Any additional spherical curvature of the anode foil simply adds to this natural self-focusing in a manner similar to simple geometric optics. This self-focusing is in contrast to the conventional PRD where the self-magnetic field from the ion current leads to a nearly constant bending angle which must be compensated for by an aspheric focusing anode foil.

The other major difference and advantage of the EPRD over the conventional PRD is that the ratio of ion current to electron current, I_i/I_e, is decoupled from the diode impedance Z. In contrast, in a conventional PRD I_i/I_e scales like R/D and Z scales like D/R, which leads to high ion efficiency only for low impedance diodes (i.e., $R/D \gg 1$). For a given anode-cathode gap spacing, D, and diode radius, R, the impedance of the EPRD is proportional to D/R as with the conventional PRD, however, I_i/I_e is proportional to H/D (i.e., the electron path length/the ion path length) and is independent of diode radius or diode impedance. Theoretically, for any current equal to or above the critical current, the ion production efficiency can be made arbitrarily large by increasing the separation between the two disc cathodes. These properties were verified using a particle-in-cell code.

The EPRD has been tested on Gamble II by driving only the upper half of the diode shown in Fig. 4 in a coaxial-feed geometry.[3,8] The diode was designed for negative-polarity operation of Gamble II to allow optical alignment. This arrangement required diagnostic connections through transit-time-isolator cables installed in the coaxial water line. The anode radius was 7 cm and anode lengths of 5, 10 and 15 cm have been used to provide configurations where the electron path length in the diode was respectively less than, comparable to, and greater than the diode radius. Typical anode-cathode gaps were 3.5 to 6 mm. Diagnostics included x-ray pinhole cameras, probes for measurement of net ion current, total diode current and diode voltage, arrays of ion collector probes, ion beam pinhole imaging to determine beam uniformity, direction and divergence, and

various witness plate configurations.

Initial experiments have shown the diode to be an efficient ion source and a good electrical match to the accelerator. Net ion currents on the order of 400 kA have been measured with diode impedances of 1.5-2 Ω. The diode impedance has been shown to be a linear function of anode-cathode gap but practically independent of diode axial height as predicted by theory. Definite limits to the anode surface area which can be uniformly turned on at a given diode power level have been observed. Nearly azimuthally-symmetric electron and ion current flow has been observed. Filamentation of mode number ~ 100 has been observed at the cathode with concomitant filamentation with mode number ~ 10 in the electron flow down the anode. Somewhat higher ion production enhancements have been observed from anode areas containing these filaments. Imaging of ion beamlets shows time-averaged half-angle divergence of 1-2° from areas not containing filaments while ions from filamented areas have 10-15° time-averaged half-angle divergences, principally in the azimuthal direction. Experiments to reduce the beam filamentation are in progress. SNL is presently testing a high power diode of similar design on PBFA I.[9]

IV. INDUCTIVE STORAGE APPROACH

Experiments are presently in progress at NRL[10,25] to test the concept of using vacuum inductive storage techniques with fast plasma opening switches (POS). Eventually this system is intended for use in compressing the pulse duration of the outputs of PBFA I and II from the present 40 ns to 10 ns. Techniques similar to ones employed in these experiments have been used previously for suppression of prepulse and steepening of pulse risetime on high-power generators[26] as well as in plasma-filled diode experiments.[27]

The basic approach, which is conceptually illustrated in Fig. 5 is to store magnetic energy by current charging a vacuum inductor with the output pulse from the generator. Plasma supplied by external sources provide a low impedance path and shunts the current (I_s) from the diode load (R_L) during the charging time. The plasma parameters are chosen so that before the peak of the charging current, a gap near the cathode forms and a bipolar Child-Langmuir diode is established with a self-generated cathode plasma on one side and the injected plasma acting as an anode on the other (Fig. 5b). The ion flux from the plasma anode which must be sufficient to maintain bipolar flow across the plasma-gap interface is provided by eroding the plasma and opening the gap. This erosion can produce opening velocities of ~ 10 cm/μs. As the gap, D, increases, the Child-Langmuir switch impedance increases (proportional to D^2) giving an increasing switch resistance. During this time the generator charging voltage continues to increase thus further increasing the current in the switch region. At high enough current levels the switch electrons are bent downstream by their self-magnetic field

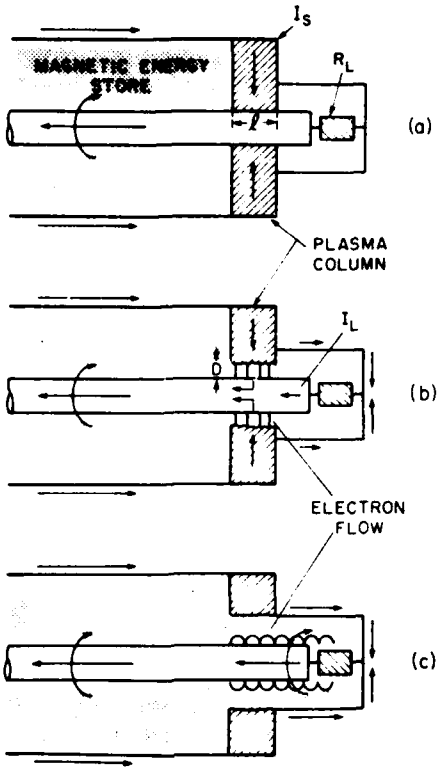

Fig. 5. Plasma opening switch stages with (a) inductor charging and switch closed (b) plasma eroding and switch opening and (c) switch opened, electron flow magnetically insulated and energy switched into load.

and travel along the plasma surface of length, ℓ. The ion flux, and therefore the erosion rate, is thus increased by a factor of ℓ/D in the same way as the ion current in a pinched-beam ion diode[6,28] is enhanced. Opening velocities of ~ 100 cm/μs are possible with this enhancement, leading to a very fast increase in switch resistance. As the switch impedance increases, the load begins to conduct a larger fraction of the current. When the diode current (I_L) exceeds the critical current for magnetic insulation in the switch gap, the electrons no longer interact with the plasma and travel down the final section of transmission line to the load (Fig. 5c).

In the preliminary NRL experiments,[10] to be described below, energy from a pulsed power accelerator is first stored in a vacuum inductor and then extracted through a low inductance, high impedance load. Results show the POS remains closed for up to 70 ns as the vacuum inductor is charged and then opens in < 10 ns. Most of the energy in the inductor is then delivered to an electron-beam diode load. Voltage increases of a factor of

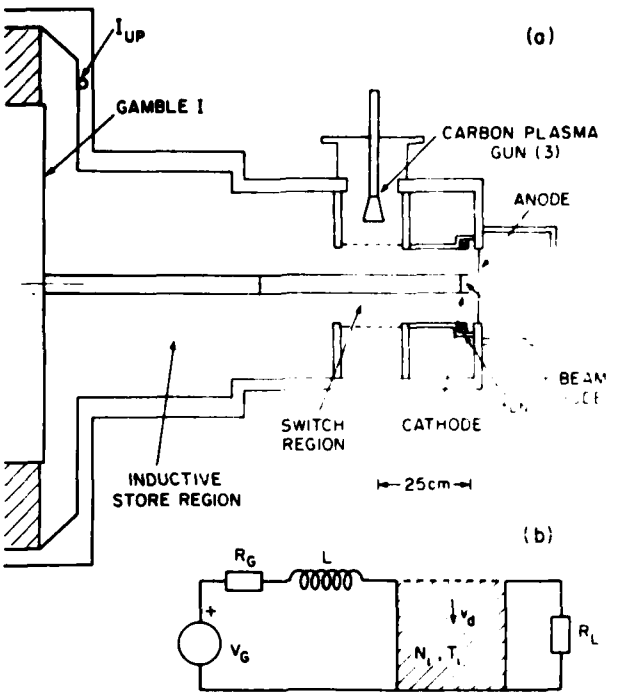

Fig. 6. Schematic of (a) Gamble I plasma opening switch (POS) experiment and (b) equivalent circuit.

two and power multiplications of up to a factor of four over non-POS shots have been measured.

In these experiments the NRL Gamble I accelerator with an effective 2 Ω output generator impedance was used to charge a coaxial vacuum inductor with a negative 1 MV, 60 ns, FWHM sinusoidal open circuit voltage waveform. Figure 6 shows a schematic of the experiment and an equivalent circuit diagram. The ~ 140 nH, high impedance vacuum inductor section and the ~ 35 nH insulator provide the L_S ~ 175 nH inductive store. The switch section contains three carbon plasma guns of a type previously used at SNL.[29] A 6 cm diameter hollow cylindrical aluminum cathode with a 1 cm anode-cathode gap spacing was used as an ~ 12 Ω electron-beam diode load.

Diagnostics included a voltage monitor upstream of the Gamble I insulator, a current monitor in the inductor section labeled I_{UP} and another current monitor downstream of the switch region labeled I_{DN}. A photodiode with a plastic scintillator to measure x-rays was located on axis 35 cm downstream of the anode.

Shown in Fig. 7 is experimental data from two shots, one with the POS and one without. The currents in the inductor, I_{UP}, and in the electron-beam load section, I_{DN}, are shown in Fig. 7a. Without the POS the accelerator sees the inductance in series with

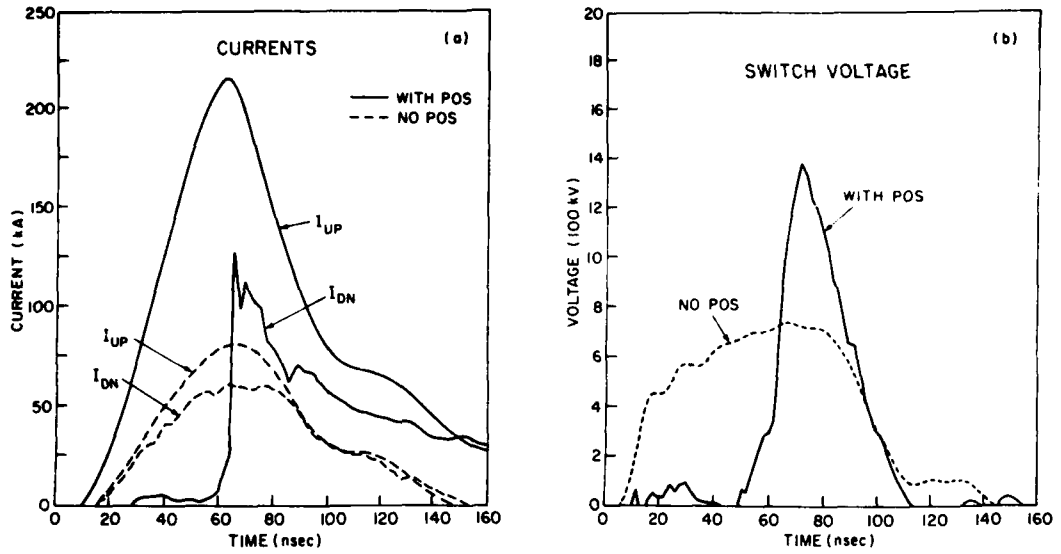

Fig. 7. Output traces of (a) currents and (b) switch voltage for shots with and without a POS.

the ~ 12 Ω electron-beam load. This limits the peak current in the inductor to ~ 80 kA. I_{DN} follows I_{UP} with some current loss due to cathode stalk emission. With the POS the accelerator sees only the inductive store and the closed switch for the first ~ 50 ns. During this time the switch diverts up to 220 kA from the load. When the switch begins to open, the downstream current rises to $\gtrsim$ 130 kA in ~ 6 ns with a maximum $dI_{DN}/dt \sim 2.2 \times 10^{13}$ A/s. The observed rapid opening is attributed to self-magnetic-field effects in the switch resulting in the ℓ/D enhancement of the ion current flowing out of the switch. An apparent loss of 90 kA occurs in the switch-to-load region. This loss is partially in the form of intense beamlets striking the outer conductor just downstream of the switch region and represents a shunt resistance even when the switch has opened. If this loss is related to the geometry of the short line downstream of the switch not properly retrapping the switch electron flow, then, in principle, it could be minimized in future experiments.

The voltage across the switch, which is approximately the same as the voltage across the load, was computed from the measured insulator voltage, V_D, and dI_{UP}/dt, and is shown in Fig. 7b. The FWHM of the voltage pulse with the POS is reduced by a factor of three and the peak voltage is a factor of two higher than without the POS. The x-ray signals (not shown) agree with the pulse compression and voltage multiplication.

The peak power into the switch and load combination is 0.065 TW without the POS and 0.28 TW with the POS. The four-fold increase in peak power results from the higher voltage and current obtained with the switch. For comparison, the power delivered to a matched (2 Ω) low inductance (30 nH) diode is 0.14 TW for a similar accelerator pulse.

Many shots were taken with different plasma densities in the switch region and with different timings between the arrival of the plasma in the switch region and the arrival of the accelerator pulse. The switch opening was observed to be reproducible within the limits of the plasma gun and accelerator pulse reproducibility. The switch could be made to divert only the leading edge of the accelerator pulse as desired for prepulse suppression or to divert as much as 250 kA with the switch still opening in ~ 10 ns depending on how much plasma was injected. If too much plasma was injected, the switch diverted the entire pulse from the load. An extended parameter study of density effects is presently being performed.

Similar experiments are presently being carried out on Gamble II in order to scale the previous results to higher currents (1 MA) and energies (50 kJ). If they are successful, these techniques will first be tested on a single module of SANDIA's PBFA I in 1983 and then on the entire generator during 1984. If by using these techniques the PBFA I output pulse length could be shortened while increasing the voltage and power, it might be possible to perform significant pellet physics experiments with light-ions even before PBFA II is completed in 1986. If the initial PBFA I experiments are successful, this approach will be applied to PBFA II. Very preliminary studies suggest that using this approach PBFA II could deliver up to 400 TW at 30 MV in 10 ns to a small diameter high impedance ion diode.

V. ENERGY LOSS EXPERIMENT

Theoretical research[30] indicates that, at the ionization levels of ICF pellet plasmas, the stopping power of light ions may be enhanced by a factor of two over that in a cold target. In this section, measurements of the energy loss of MeV deuterons in plasmas formed by focusing intense Gamble II ion beams[15] (1 MeV, 0.2 MA, 20 ns) onto subrange-thick targets are presented. The short 20 ns proton pulse duration is achieved by allowing the diode water-vacuum interface to flash over on the vacuum side just after peak voltage. The results demonstrate that the stopping power of the heated target is enhanced over that of the cold target.

For these energy-loss measurements, a spherically-contoured PRD is used to produce a 250 kA/cm^2 focused deuteron beam while a planar anode foil version of the diode is used to produce a 50 kA/cm^2 deuteron beam. The 0.01 cm thick plastic anode foil is coated with deuterated polyethylene (CD_2) to provide the deuterons.

The experimental technique for determining the deuteron energy loss uses neutron time-of-flight (TOF) with a multi-layered target. The target consists of a subrange stopping foil sandwiched between 0.3-μm and 1.0-μm thick layers of CD_2. Measurements of the d-d neutron TOF from the two CD_2 targets are used to determine both the incident deuteron energy and the

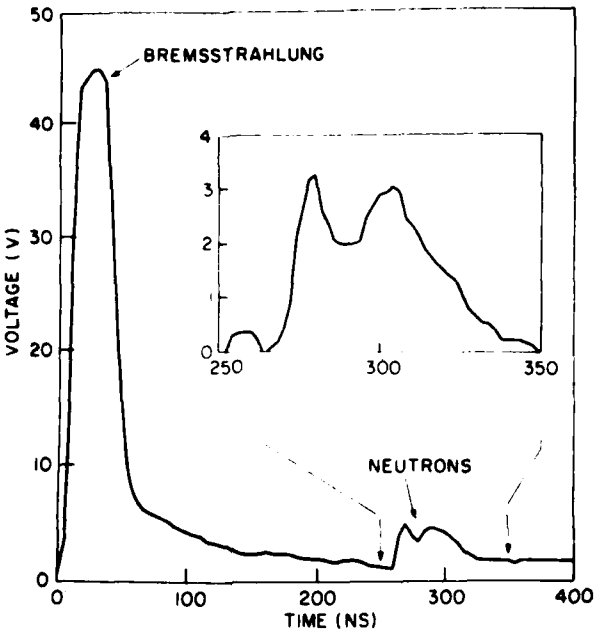

Fig. 8. Neutron time-of-flight trace with bremsstrahlung background subtracted from insert.

deuteron energy loss in the stopping foil on each shot. The thickness of the stopping foil is adjusted so that neutrons from the two CD_2 targets can be resolved. In these experiments, 6.4-μm thick Mylar and aluminum stopping foils are used. Fig. 8 shows a typical trace from the neutron TOF detector. The time interval between the peak of the ion power and the peak of the first neutron pulse determines the neutron energy from the front CD_2 target and, by kinematic calculation, the incident deuteron energy. The time separation of the two neutron peaks provides a direct measure of the deuteron energy loss in the stopping foil.

The results of stopping-power measurements using both planar and spherical diodes are presented in Fig. 9. For each case, the measurements are compared to the cold-target energy loss deduced from measurements of stopping cross sections by Andersen and Ziegler.[31] The measured energy losses are significantly larger than cold-target values in all cases except for the planar diode with a Mylar target. In this case, the measurements are consistent with cold-target values.

The deuteron energy losses deviate from that in a cold target when sufficient ionization occurs in the stopping medium. Hydrocode calculations which model this experiment[16] indicate that the target has expanded to about 2-mm thickness at the peak of the power pulse, and that the electron temperature is 4 to 5 eV at 50 kA/cm^2 and 13 to 17 eV at 250 kA/cm^2 for an aluminum stopping foil. Similar results for Mylar are ~3 eV at 50 kA/cm^2 and 9 to 11 eV at 250 kA/cm^2. The calculated energy losses at peak power are shown as solid triangles in Fig. 9 and are in reasonable

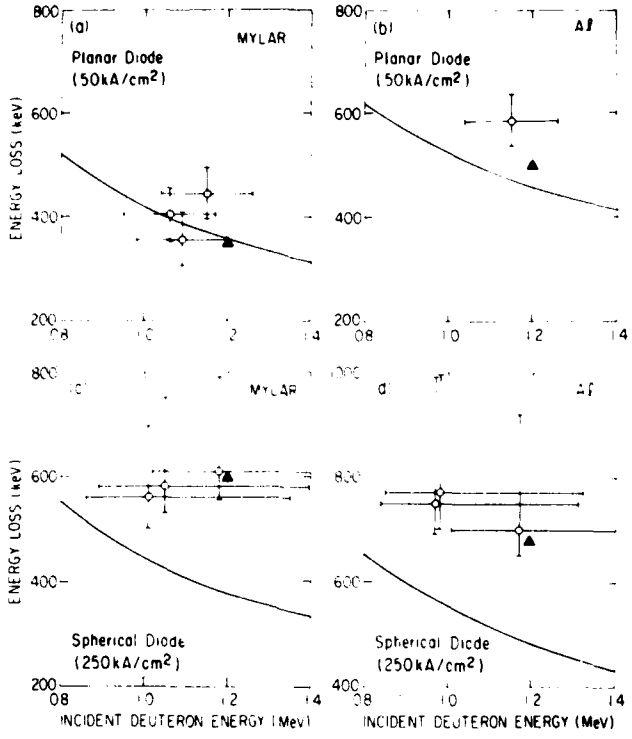

Fig. 9. Data from energy-loss experiment.

agreement with the measurements. For the experimental conditions where a significant number of free electrons are produced in the stopping foil, the measured deuteron stopping is enhanced (Figs. 9b, c and d). If the energy deposition produces less ionization, the measured energy loss is consistent with cold-target stopping (Fig. 9a).

VI. FUTURE PLANS

Research results on various aspects of the modular approach to light-ion ICF are encouraging and suggest that this approach could lead to pellet ignition experiments and eventually to a reactor scenario. However, for the PRDs presently being considered, the needed bunching factor of 3 to 4 requires a ramped voltage waveform on the diode. This requirement inherently leads to inefficient use of the energy stored in the pulsed power generator. A possible solution is to use a plasma-filled PRD whose impedance can be made to increase during the power pulse, thus providing the required voltage waveshape. This solution requires more research, but fortunately could draw on both the research at SNL on plasma-filled diodes[32] and the research at NRL on plasma opening switches.

The single diode approach, using either the NRL EPRD described herein, or the SNL applied-B or AMPFION-HYBRID diodes described elsewhere,[2] also show encouraging results. This approach may be less complicated than the modular approach in that there are no transport channels. This approach is also more compatible with the SNL imploding foil approach[2] to ICF on PBFA II because both require the generator energy to be delivered to a single, small diameter load. PBFA II could be operated at low voltage (2-4 MV) for protons or deuterons, or at high voltages (15-30 MV) to obtain higher brightness with higher atomic weight ions such as singly-charged lithium. In either case, the long 35 ns pulse duration leads to low power densities on target which require complex pellet design and lead to fabrication difficulties. If the SNL plasma-filled AMPFION diode[32] properly scales to PBFA II parameters, then the inherent bunching which occurs with such a diode leads to shorter pulses and higher power densities. This beam could then be delivered to a simple pellet with a single diode approach.

Power gain through inductive storage and switching in vacuum using plasma opening switches as described herein could help to solve many of the previously mentioned problems. Such an auxiliary stage on the output of PBFA II could reduce the pulse duration delivered to a diode to 10 ns. This would allow the use of smaller anode-cathode gap spacings making it easier to use a small diameter diode. This, in combination with the higher brightness obtained from the higher voltage and higher atomic weight ions, would lead to significantly higher power densities on target, thus considerably simplifying the target design. However, problems still remain to be solved, such as switch synchronization between several modules, and efficient coupling of the energy stored in the inductor into the load.

It should be noted that, if switch synchronization can be obtained, this inductive storage and vacuum switching approach can also be applied to the modular approach. The short pulse would eliminate the need for the voltage ramp, make it easier to drive a small diameter, high brightness diode, and relax many of the constraints on ion transport. The stand-off achieved with transport would allow for the future development of a reactor system. The required final-focusing section could, in principle, be made a disposable part of the pellet structure with external currents supplied through laser channels.

At present, the priority in the NRL Light-Ion ICF Program is to support SNL in the achievement of pellet ignition on PBFA II. This requires that our limited program resources be concentrated on fewer approaches. In the near term, NRL will emphasize vacuum inductive storage with plasma opening switches as applied to the single diode approach. Research on obtaining high brightness ion beams will also continue, but with emphasis on using short, high voltage pulses to drive the diodes. These short pulses may require the development of either active anode and/or cathode plasmas. The modular approach involving transport and final

focusing will be given lower priority until some appropriate time in the future when initial pellet ignition experiments will have been performed.

VII. REFERENCES

1. P.A. Miller, Bull. Am. Phys. Soc. 27, 1094 (1982).
2. G. Yonas, in Proceedings of the 9th Int. Conf. on Plasma Phys. and Cont. Nucl. Fus. Res., Baltimore, MD (1982); G. Yonas and J.P. VanDevender, these proceedings.
3. G. Cooperstein, R.J. Barker, D.G. Colombant, A. Drobot, S.A. Goldstein, R.A. Meger, D. Mosher, P.F. Ottinger, F.L. Sandel, S.J. Stephanakis and F.C. Young, in the Proceedings of the 9th Int. Conf. of Plasma Phys. and Cont. Nucl. Fus. Res., Baltimore, MD (1982).
4. F.L. Sandel, S.J. Stephanakis, F.C. Young and W.F. Oliphant, in the Proceedings of the 4th Int. Conf. on High-Power Electron- and Ion-Beam Research and Technology, Palaiseau, France (1981), p. 129; G. Cooperstein, S.A. Goldstein, R.A. Meger, D. Mosher, W.F. Oliphant, F.L. Sandel, S.J. Stephanakis, F.C. Young, and H.U. Karow, ibid., p. 53; J.N. Olsen and R.J. Leeper, J. Appl. Phys. 53, 3397(1982); see also C.L. Olson, J. of Fusion Energy 1, 309(1982).
5. S.A. Goldstein, D.G. Colombant, D. Mosher, P.F. Ottinger and F.L. Sandel, ibid., p. 113; D. Mosher, D.G. Colombant, S.A. Goldstein and P.F. Ottinger, ibid., p. 19; P.F. Ottinger, S.A. Goldstein and D. Mosher, 1980 IEEE Int. Conf. on Plasma Science, Madison, Wisconsin (1980), p. 95.
6. G. Cooperstein, S.A. Goldstein, D. Mosher, R.J. Barker, J.R. Boller, D.G. Colombant, A. Drobot, R.A. Meger, W.F. Oliphant, P.F. Ottinger, F.L. Sandel, S.J. Stephanakis and F.C. Young, in Laser Interaction and Related Plasma Phenomena, edited by H. Schwarz, H. Hora, M. Lubin and B. Yaakobi (Plenum, New York, 1981), Vol. 5, p. 105.
7. P.F. Ottinger, S.A. Goldstein and D. Mosher, NRL Memo Report 4948, November 1982; D. Mosher, D.G. Colombant and S.A. Goldstein, Comments Plasma Physics, 6, 101 (1981).
8. F.L. Sandel, private communication; R.J. Barker and S.A. Goldstein, Bull. Am. Phys. Soc. 26, 921 (1981).
9. J.N. Olsen, S.E. Rosenthal, L.P. Mix, R.J. Leeper, R.J. Anderson, P.L. Dreike, D.B. Seidel, J.P. Quintenz and J.W. Poukey, Bull. Am. Phys. Soc. 27, 1120 (1982).
10. R.A. Meger, R.J. Commisso, G. Cooperstein and S.A. Goldstein, Appl. Phys. Lett. 42, 943(1983).
11. S.J. Stephanakis, S.A. Goldstein, P.F. Ottinger, D. Mosher, Bull. Am. Phys. Soc. 26, 921 (1981).
12. R.A. Meger, S. A. Goldstein, P.F. Ottinger, D. Mosher, S.J. Stephanakis, and F.C. Young, Bull. Am. Phys. Soc. 26, 921 (1981).
13. P.F. Ottinger, D.G. Colombant, S.A. Goldstein, R.A. Meger and D. Mosher, ibid.
14. C.W. Mendel, Jr. and S.A. Goldstein, J. Appl. Phys. 48, 4004 (1977); P.A. Miller, J.W. Poukey and T.P. Wright, Phys. Rev.

Lett. 35, 940(1975).
15. F.C. Young, D. Mosher, S.J. Stephanakis and S.A. Goldstein, Phys. Rev. Lett. 49, 549 (1982).
16. T.A. Mehlhorn, private communication.
17. J.W. Maenchen, F.C. Young, R. Stringfield, S.J. Stephanakis, D. Mosher, S.A. Goldstein, R.D. Genuario and G. Cooperstein, J. Appl. Phys. 54, 89(1983); F.C. Young, G. Cooperstein, S.A. Goldstein, D. Mosher, S.J. Stephanakis, W.F. Oliphant, J.R. Boller, J. Maenchen, R.D. Genuario and R.N. Stringfield, NRL Memorandum Report 4726 (1981).
18. P.F. Ottinger, S.A. Goldstein, J. Guillory and V.K. Tripathi, Bull. Am. Phys. Soc. 27, 1121 (1982).
19. A.T. Drobot, T.M. Antonsen, W.H. Miner and E. Ott, ibid., p. 991.
20. D.G. Colombant and S.A. Goldstein, ibid., p. 1124.
21. S.J. Stephanakis, S.A. Goldstein, R.J. Barker, J.R. Boller and G. Cooperstein, ibid., p. 992; R.J. Barker, S.A. Goldstein, S.J. Stephanakis and G. Cooperstein, ibid., p. 991.
22. J.N. Olsen, and R.J. Leeper, J. Appl. Phys. 53, 3397 (1982).
23. D.G. Colombant, D. Mosher and S.A. Goldstein, Phys. Rev. Lett. 45, 1253 (1980); D.G. Colombant and S.A. Goldstein, NRL Memorandum Report 4640 (1981).
24. P.F. Ottinger, D. Mosher and S.A. Goldstein, Phys. Fluids 22, 332 (1979); P.F. Ottinger, D. Mosher and S.A. Goldstein Phys. Fluids 24, 164 (1981).
25. R.A. Meger, R.J. Barker, R.J. Commisso, G. Cooperstein, S.A. Goldstein, J.M. Neri and P.F. Ottinger, Bull. Am. Phys. Soc. 27, 991 (1982); J.M. Neri, R.J. Commisso and R.A. Meger, ibid., p. 1054.
26. C.W. Mendel, Jr. and S.A. Goldstein, J. Appl. Phys. 48, 1004 (1977); R. Stringfield, R. Schneider, R.D. Genuario, I. Roth, K. Childers, C. Stallings and D. Dakin, J. Appl. Phys. 52, 1278 (1981); R. Richardson, E. Brown, J. Pearlman, to be published; R.A. Meger and F.C. Young, J. Appl. Phys. 53, 8543 (1982); R.A. Meger and F.C. Young, NRL Memorandum Report 4838, June, 1982.
27. P.A. Miller, J.W. Poukey and T.P. Wright, Phys. Rev. Lett. 35, 940 (1975).
28. S.A. Goldstein and R. Lee, Phys. Rev. Lett. 35, 1079 (1975).
29. C.W. Mendel, Jr., D.M. Zagar, G.S. Mills, S. Humphries, Jr. and S.A. Goldstein, Rev. Sci. Instrum. 51, 1641 (1980).
30. T.A. Mehlhorn, J. Appl. Phys. 52, 6522 (1981); E. Nardi, E. Peleg and Z. Zinamon, Appl. Phys. Lett. 39, 46 (1981); D. Mosher in ERDA Summer Study of Heavy Ions for Inertial Fusion LBL-5543, 1976, p. 39 (unpublished).
31. H.H. Andersen and J.F. Ziegler, The Stopping and Ranges of Ions in Matter, Vol. 3 (Pergamon Press, NY 1977).
32. C.W. Mendel, Jr., P.A. Miller, J.P. Quintenz, D.B. Seidel and S.A. Slutz, in the Proceedings of the 4th Int. Topical Conf. on High-Power Electron- and Ion-Beam Research and Technology, Palaiseau, France (1981) p. 45; C.W. Mendel, Jr. and G.S. Mills, to be published in J. Appl. Phys.

DISTRIBUTION LIST

Director
Defense Nuclear Agency
Washington, DC 20305
Attn: TISI Archieves 1 copy
FITL Tech. LIbrary 3 copy
J. Z. Farber (RAEV) 1 copy
H. Soo (RAEV) 1 copy
J. Benson (RAEV) 1 copy

U.S. Department of Energy
Division of Inertial Fusion
Washington, DC 20545
Attn: L. E. Killion 1 copy
S.L. Kahalas 1 copy
R.L. Schriever 1 copy

U.S. Department of Energy
Office of Classification
Washington, DC 20545
Attn: Robert T. Duff 1 copy

U.S. Department of Energy
Nevada Operations Office
Post Office Box 14100
Las Vegas, NV 89114
Attn: Rex Purcell 2 copies

U.S. Department of Energy
P.O. Box 62
Oak Ridge, TN 37830 2 copy

Air Force Office of Scientific Research
Physics Directorate
Bolling AFB, DC 20332
Attn: A. K. Hyder 1 copy
M. A. Stroscio 1 copy

Air Force Weapons Laboratory, AFSC
Kirtland AFB, NM 87117
Attn: NTYP (W. L. Baker) 1 copy

Atomic Weapons Research Establishment
Building H36
Aldermaston, Reading RG 7 4PR
United Kingdom
Attn: J.C. Martin 1 copy

Boeing Company, The
P.O. Box 3707
Seattle, WA 98124
Attn: Aerospace Library 1 copy

Brookhaven National Laboratory
Upton, NY 11973
Attn: A.F. Maschke 1 copy

BMO/EN
Norton AFB, CA
Attn: ENSN 1 copy

Commander
Harry Diamond Laboratory
2800 Powder Mill Rd.
Adelphi, MD 20783
(CNWDI-INNER ENVELOPE: ATTN: DELHD-RBH)
Attn: DELHD-NP 1 copy
DELHD-RCC -J.A. Rosando 1 copy
DRXDO-RBH - K. Kerris 1 copy
DRXDO-TI - Tech Lib. 1 copy

Cornell University
Ithaca, NY 14850
Attn: D.A. Hammer 1 copy
R.N. Sudan 1 copy

Defense Advanced Research Project Agency
1400 Wilson Blvd.
Arlington, VA 22209
Attn: R. L. Gullickson 1 copy

Defense Technical Information Center
Cameron Station
5010 Duke Street
Alexandria, VA 22314
Attn: T.C. 2 copies

JAYCOR, Inc.
205 S. Whiting Street
Alexandria, VA 22304
Attn: J. Guillory 1 copy

Kaman Tempo
816 State Street (P.O. Drawer QQ)
Santa Barbara, CA 93102
Attn: DASIAC 1 copy

KMS Fusion, Inc.
3941 Research Park Drive
P.O. Box 1567
Ann Arbor, MI 48106
Attn: Alexander A. Glass 1 copy

Lawrence Berkeley Laboratory
Berkeley, CA 94720
Attn: D. Keefe 1 copy

Lawrence Livermore National Laboratory
P.O. Box 808
Livermore, CA 94550
Attn:
Tech. Info. Dept. L-3 1 copy
D.J. Mecker 1 copy
R.E. Batzel/J. Kahn,L-1 1 copy
J.L. Emmett, L-488 1 copy
J.F. Holzrichter, L-481 1 copy
W.F. Krupke, L-488 1 copy
J.H. Nuckolls, L-477 1 copy

Los Alamos National Laboratory
P.O. Box 1663
Los Alamos, NM 87545
Attn: M. Gillispie/Theo.Div. 1 copy
S.D. Rockwood,ICF Prog. Mgr.
DAD/IF M/S 527 6 copies

Massachusetts Institute of Technology
Cambridge, MA 02139
Attn: R.C. Davidson 1 copy
G. Bekefi 1 copy

Maxwell Laboratories, Inc.
9244 Balboa Avenue
San Diego, CA 92123
Attn: J.Pearlman 1 copy

Mission Research Corporation
1400 San Mateo Blvd. SE
Albuquerque, NM 87108
Attn: B.B. Godfrey 1 copy

National Science Foundation
Mail Stop 19
Washington, DC 20550
Attn: D. Berley 1 copy

Naval Research Laboratory
Addressee: Attn: Name/Code
Code 2628 -TID Distribution 20 copies
Code 4000 - T. Coffey 1 copy
Code 4040 - J. Boris 1 copy
Code 4700 - S.L. Ossakow 26 copies
Code 4704 - C. Kapetanakos 1 copy
Code 4720 - J. Davis 1 copy
Code 4730 - S. Bodner 1 copy
Code 4740 - V. Granatstein 1 copy
Code 4760 - B. Robson 1 copy
Code 4770 - I.M. Vitkovitsky 10 copies
Code 4771 - F. C. Young 1 copy
Code 4773 - G. Cooperstein 10 copies
Code 4773 - S.J. Stephanakis 1 copy
Code 4790 - D. Colombant 1 copy
Code 4790 - I. Haber 1 copy
Code 4790 - M. Lampe 1 copy
Code 6682 - D. Nagel 1 copy
Code 4770 400 copies

Office of Naval Research
London Branch Office
Box 39
FPO New York, NY 09510
Attn: Dr. David Mosher 1 copy

Physics International Co.
2700 Merced Street
San Leandro, CA 94577
Attn: A.J. Toepfer 1 copy

Pulse Sciences, Inc.
1615 Broadway, Suite 610
Oakland, CA 94612
Attn: S. Putnam 1 copy

R&D Associates
Suite 500
1401 Wilson Blvd.
Arlington, VA 22209
Attn: P.J. Turchi 1 copy

R&D Associates
P.O. Box 9695
Marina Del Rey, CA 90291
Attn: C. MacDonald 1 copy

Sandia National Laboratories
P.O. Box 5800
Albuquerque, NM 87185
Attn: P.Vandevender / 1260 6 copies

Spire Corporation
P.O. Box D
Bedford, MA 01730
Attn: R.G. Little 1 copy
Stanford University
SLAC
P.O. Box 4349

Stanford, CA 94305
Attn: W.B. Herrmannsfeldt 1 copy

University of California
Irvine, CA 92717
Attn: N. Rostoker 1 copy

University of Rochester
250 East River Road
Rochester, NY 14623
Attn: J. Eastman 1 copy

Univ. of Washington
Dept. of Nuclear Engineering
BF-10
Seattle, WA 98115
Attn: F. Ribe 1 copy

END

FILMED

1-84

DTIC